Electrochemical and Solid-State Letters, **13** (12) H403-H405 (2010)
1099-0062/2010/13(12)/H403/3/$28.00 © The Electrochemical Society

Schottky Barrier Characteristics and Carrier Transport Mechanism for Ohmic Contacts to Strained p-Type InGaN/GaN Superlattice

Sun-Ho Jang and Ja-Soon Jang[*,z]

Department of Electronic Engineering, LED-IT Fusion Technology Research Center, Yeungnam University, Gyeongbuk 700-712, Korea

We report on the metal work function dependence on Schottky barrier characteristics and the carrier transport mechanism for ohmic contacts to strained p-InGaN/GaN superlattices. Measurements showed that specific contact resistances are dependent on metal work functions, whereas Schottky barrier heights exhibit relatively little dependency on metal work functions. These indicate that the overall contact properties are directly affected by polarization-induced carriers near the surface of the strained InGaN. The carrier conduction mechanism for the contacts to the InGaN/GaN is described in terms of tunneling or compensation effect, depending on temperatures.
 [DOI: 10.1149/1.3486447]

Manuscript submitted April 12, 2010; revised manuscript received August 13, 2010. Published September 13, 2010.

Low resistance ohmic contacts are essential to achieve the high formance of GaN-based devices. In particular, for p-type GaN, to the absence of metals having a work function larger than eV and the difficulty of obtaining high carrier concentrations 10^{18} cm^{-3}), it was difficult to achieve ohmic contacts to p-GaN ing a specific contact resistance less than 10^{-4} Ω cm^2.[1] Among reported various approaches to realize low specific contact resistces to p-GaN,[2-10] a method using strain-induced polarization lay- such as p-type AlGaN/p-GaN superlattice (SL) and p-InGaN/p-N is very effective in improving p-ohmic properties.[7-9] Strain-uced piezoelectric effect (PE) as well as spontaneous polarization P) in the polarization field-induced (PFI) layer give rise to a high e density near the sample surface by forming a two-dimensional e gas. In these schemes having PE and SP, high concentrations 10^{18} cm^{-3}) increase a hole-tunneling probability at the interface ween contact schemes and strained layers, and hence, result in specific contact resistance.[7,9,10] Recently, indium tin oxide mic contacts to strained p-InGaN/GaN having excellent thermal bility as well as low specific contact resistance had been successly demonstrated.[11] Annealing leads to the formation of In–Ga–O/ GaN (at the interface), acting as a diffusion barrier able to prevent formation of nitrogen vacancies and the indiffusion of Sn atoms o InGaN/GaN, which are detrimental to the formation of p-type mic contact.

However, detailed studies of Schottky barrier characteristics and rier transport mechanisms for ohmic contacts to strained p-type GaN/p-GaN SLs have not extensively hitherto performed despite ir technological importance. In this article, we have investigated Schottky barrier height (SBH) dependence on the metal work ction and specific contact resistance. Possible carrier transport chanisms of ohmic contacts to the InGaN/GaN have also been estigated using the relation between specific contact resistance d temperature. The overall contact-performance characteristics are siderably dependent on PFI carriers near the InGaN surface in- d of different metal work functions. Also, there is a wide tem- ature range within which temperature-independent tunneling nsport dominates.

A metallorganic chemical vapor deposition system was used to w a 2 μm thick, unintentionally doped GaN layer on a 30 nm k GaN nucleation layer/(0001) sapphire substrate. This was fol- ed by the growth of 100 nm thick p-GaN:Mg and then a 3 nm k, p-type $In_{0.15}Ga_{0.85}N$ layer/a 3 nm thick p-GaN/a 3 nm thick $In_{0.15}Ga_{0.85}N$ layer were grown on p-GaN. Secondary-ion mass ctroscopy (SIMS) measurement showed that the Mg concentra- n of both p-GaN and p-InGaN was 1.2×10^{19} cm^{-3}. Before the fabrication of circular transmission line model (CTLM) patterns, the surface of the InGaN/GaN layer was ultrasonically degreased with acetone, methanol, and ethanol for 5 min in each step, and then rinsed with deionized water. The CTLM patterns were defined on the surface-treated InGaN/GaN using a photolithographic technique. The inner radius of the CTLM pad was 110 μm and the spacings between the inner and outer pads were 5, 10, 15, 20, 25, and 35 μm. Before the deposition of metal films, the CTLM-patterned layers were dipped into a buffered oxide etch solution for 60 s. Ti, Cr, Ni, and Pt were then deposited by an electron-beam evaporation. Specific contact resistances (R_{sc}) and specific contact resistance–temperature (R_{sc}-T) were obtained using a semiconductor analyzer (HP 4155A) and a hot chuck system.

For the contacts to polarization field-free (PFF) p-InGaN/GaN, SBH ($q\Phi_B$) can be basically obtained using the relation given by[12]

$$q\Phi_B = E_{g,InGaN} - q(\Phi_M - \chi_{InGaN}) \quad [1]$$

where $q\Phi_M$ is the metal work function, E_g is the bandgap energy, and χ is the electron affinity. The ternary bandgap energy and affinity of the InGaN capping layer can be obtained using equations given as[12]

$$E_{g,In_xGa_{1-x}N} = xE_{g,InN} + (1-x)E_{g,GaN} - bx(1-x) \quad [2]$$

$$\chi_{In_xGa_{1-x}N} = x\chi_{InN} + (1-x)\chi_{GaN} \quad [3]$$

where the E_g of InN and GaN is 0.65 and 3.3 eV at 300 K, respectively.[12] The b is the bowing parameter of 1.4 eV.[12] Using the relations 1-3, the SBHs of Ti, Cr, Ni, and Pt contacts on the p-InGaN/GaN were calculated to be 1.95, 1.75, 1.15, and 0.65 eV, respectively.

SBHs in the PFI InGaN/GaN can be obtained using the relation between specific contact resistance (R_{sc}), SBH($q\Phi_B$), and the minimum thickness of InGaN (d_{min}), which is given as[13]

$$R_{sc}^{-1} = \left(\frac{q}{2\pi\hbar d_{min}}\right)^2 (\hbar + d_{min}\sqrt{qm_h^*\Phi_B})\exp\left(-\frac{2d_{min}}{\hbar}\sqrt{qm_h^*\Phi_B}\right) \quad [4]$$

where $\hbar$ is the Plank constant ($h/2\pi$), m_h^* is the effective hole mass, N_s^{2D} is the surface charge density, and E is the electric field. d_{min} ($=\Phi_B/E = q\Phi_B/qN_s^{2D}$), the minimum thickness of the PFI InGaN, is defined as a critical thickness below which there will be no hole accumulation. At the minimum thickness, tunneling transport across the Schottky barrier occurs when a potential drop in the InGaN is equal to or larger than the SBH.[7] Specific contact resistance (R_{sc}) was determined from a plot of the measured resistances vs spacings between CTLM pads. The CTLM method was used to fit a log-scaled line to the experimental data.[14] The calculations showed

Electrochemical Society Active Member.
E-mail: jsjang@ynu.ac.kr

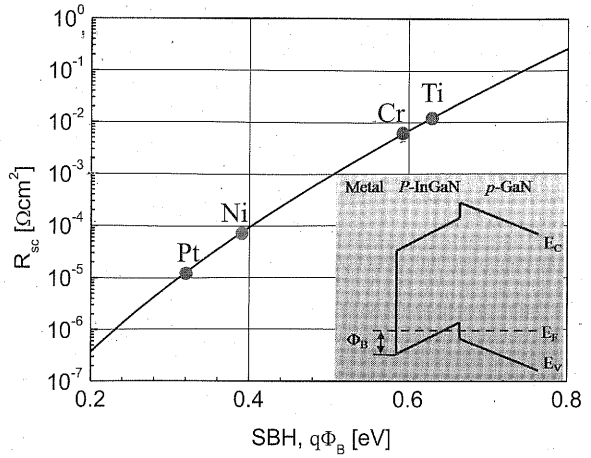

Figure 1. (Color online) Relation between specific contact resistance (R_{sc}) and SBH. In this calculation, d_{min} is 3 nm. The solid line means a theoretical result using Eq. 4. The dark circles denote the R_{sc} obtained from the CTLM method. Inset shows the possible energy band diagram at the interface between metals and p-InGaN/p-GaN.

that the R_{sc} is obtained to be $1.1(\pm 0.1) \times 10^{-2}$, $8.6(\pm 0.2) \times 10^{-3}$, $8.5(\pm 0.2) \times 10^{-5}$, and $1.3(\pm 0.2) \times 10^{-5}$ Ω cm^2 for the Ti, Cr, Ni, and Pt contacts, respectively. Using Eq. 4, the SBHs for the Ti, Cr, Ni, and Pt contacts were determined to be $0.63(\pm 0.01)$, $0.61(\pm 0.01)$, $0.39(\pm 0.01)$, and $0.31(\pm 0.01)$ eV, respectively, as shown in Fig. 1. The R_{sc} of the PFI InGaN/GaN contact is sensitively dependent on the $q\Phi_B$.

Comparisons show that the SBHs of the PFI InGaN/GaN contacts are lower than those of the PFF contacts. To understand it in detail, the $\Delta\Phi_B/\Delta\Phi_M$ factor describing metal work function dependence on SBH was introduced, as shown in Fig. 2. The theoretical $\Delta\Phi_B/\Delta\Phi_M$ value of the PFF InGaN/GaN contact is ~ 1, whereas that of the PFI contact is $\sim 0.26(\pm 0.02)$. The large difference could be due to the strain-induced PE and SP. The polarization effects in the strained InGaN/GaN produce free polarization-induced charges near the surface. The increase of the surface carrier density yields the reduction of energy band bending at the interface between metals and SLs, and consequently reduces both SBHs and contact resistivity. If we also consider the fact that a p-InGaN/GaN layer suffers from the surface Fermi-level pinning effect originating from the existence of surface defects of p-InGaN/p-GaN,[12] therefore, little

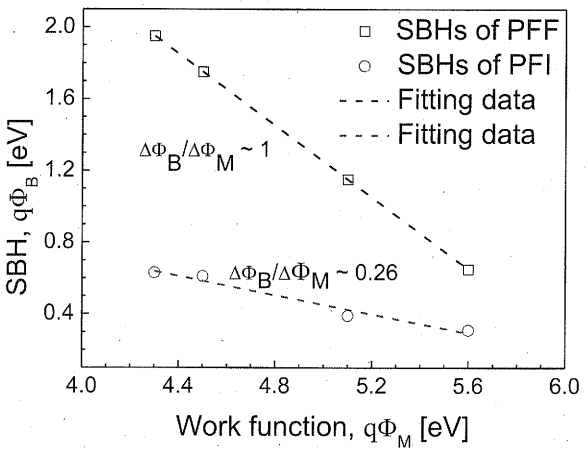

Figure 2. (Color online) Relation between SBH and metal work function. The ratio of $\Delta\Phi_B/\Delta\Phi_M$ was determined by a linear regression fitting.

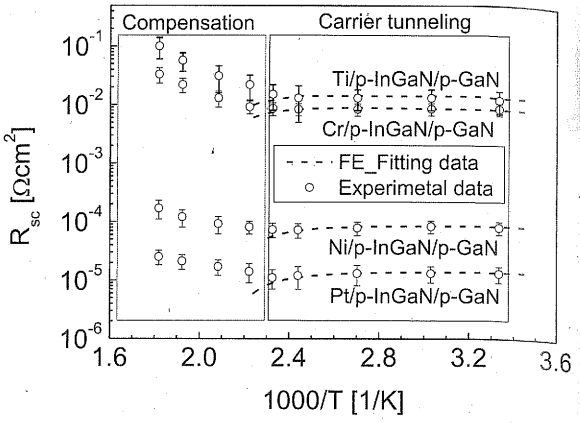

Figure 3. (Color online) Plots of the experimental and theoretical values of R_{sc} as a function of $1/T$ using a metal/p$^+$-InGaN/p-GaN model.

dependence of metal work function on the barrier height at the interface may be due to the polarization and the surface Fermi-level pinning effect.

To investigate the carrier transport mechanism at the interface, a metal/p$^+$-InGaN (a region with p-InGaN/GaN SLs)/p-GaN model [based on field emission (FE) mode] was employed.[15] Basically, a carrier distribution function in the single-strained InGaN–GaN SL is similar to the delta function. However, our scheme consists of two InGaN and GaN layers and the SIMS depth profiling (not shown here) exhibited the maximum value and exponentially decaying relation in the SL region. Thus, the carrier distribution in p$^+$-InGaN is assumed to be $N_{a\_superlattice}(x) = N_0 \exp(-x/d)$. The carrier distribution given by[15]

$$N_{total} = \frac{\int_0^d N_{a\_superlattice}(x)dx + \int_d^{t_{p\text{-}GaN}} N_{a\_p\text{-}GaN}(x)dx}{\text{Total thickness}(t)} \quad (\text{cm}^{-3}) \quad [5]$$

where d is the effective thickness of p$^+$-InGaN and $N_{a\_p\text{-}GaN}$ is the carrier concentration of p-GaN (from d to $t_{p\text{-}GaN}$). In this model, d was assumed to be the total SL thickness of 9 nm. Using Eq. 6 below, tunneling parameter (E_{00}) can be defined as $E_{00} = qh/4\pi\sqrt{N_{total}/m_h\varepsilon_s}$. The relation of FE mode is given by[15]

$$R_{sc} = \frac{k}{qA^{**}} \exp\left(\frac{q\Phi_B}{E_{00}}\right)\left[\frac{\pi T}{\sin(\pi kTC)} - \frac{\exp(-qV_pC)}{kC}\right]^{-1} \quad \text{for FE conduction} \quad [6]$$

$$C = \ln[4\Phi_B/V_p]/(2E_{00}) \quad [7]$$

where A^{**} is Richardson's constant, k is Boltzmann's constant, h is Planck's constant, m^* is the effective mass of the semiconductor, T is temperature, ε_s is the dielectric constant of the semiconductor, V_p is the energy difference of $E_F - E_V$. In this simulation (assuming an In composition of 15%), m_h of $0.84m_e$, ε_s of $10.8\varepsilon_0$, and A^{**} of 120α A cm^{-2} K^{-2} were used.[12] The α, an empirical factor, can be experimentally obtained using the thermionic emission model based on the current–voltage–temperature relation.[16] Figure 3 exhibits the plots of the experimental and theoretical values of the R_{sc} as a function of $1/T$ using a metal/p$^+$-InGaN/p-GaN model. Comparisons show that the theoretical results agree well with the experimental data, indicating that the hole flow is due to hole tunneling at $29 \leq T \leq 440$ K and our modeling is valid. This behavior can be due to the SP and PE in p-InGaN–GaN SLs, which cause high accumulated carriers near the surface. The high density of the polarization-induced charges leads to a decrease of Schottky barrier width and, hence, allows a hole-tunneling transport through the Schottky barrier. Thus, the FE conduction is dominant, irrespective of the differ

metal work function. These behaviors are fundamentally differ- from the reported results of p-GaN ohmic contacts, showing mewhat thermionic emission-like behaviors due to the low carrier ncentration of p-GaN.[16,17] However, the R_{sc} in all contacts begins increase at $T > 440$ K, indicating that all contacts suffer from rmal degradation. In particular, the degradation in the Ti and Cr ntacts becomes severe compared to others. These behaviors may related to the carrier compensation effect and interfacial reaction the interface between metal and p-SLs. Generally, surface defects the p-InGaN of the SLs occupy a relatively deep energy state, eaning that normal carriers experience some scattering and/or trap- ng with increasing T. In addition, metal–nitrides such as Ti–N and –N (in Ti- and Cr-based metallization schemes), which are detri- ental to p-ohmic contacts,[11] are thermodynamically formed at the erface because Ti–N and Cr–N phases even at room temperature ve a negative enthalpy energy of −169 and −62 kJ/mole, spectively.[18] The formation of metal–nitrides brings about a gen- ation of nitrogen vacancies (acting as a donor) in the p-InGaN and en enhances carrier compensation. Therefore, the carrier compen- ion and/or interfacial reaction may be responsible for an in- eased R_{sc} at $T > 440$ K.

In summary, we report on Schottky barrier characteristics and rrier transport mechanism at the interface between strained GaN/GaN SLs and various metals. Specific contact resistances are pendent on metal work functions, whereas SBHs exhibit relatively le dependency on metal work functions. These indicate that the erall contact properties are directly affected by polarization- uced free carriers near the surface of the strained InGaN. The le transport is closely related to tunneling or compensation effect, pending on temperatures. Our findings may serve as a design tool the formation of p-ohmic electrodes for GaN-based light emit- g diodes.

Acknowledgments

This work was supported by the Yeungnam University grant and the Korea Technology Innovation Program (grant no. 10033630) of the MKE.

Yeungnam University assisted in meeting the publication costs of this article.

References

1. S. J. Pearton, J. C. Zolper, R. J. Shul, and F. Ren, *J. Appl. Phys.*, **86**, 1 (1999).
2. T. Mori, T. Kozawa, T. Ohwaki, Y. Taga, S. Nagai, S. Yamasaki, S. Asami, N. Shibata, and M. Koite, *Appl. Phys. Lett.*, **69**, 3537 (1996).
3. J.-S. Jang, I.-S. Chang, H.-K. Kim, T.-Y. Seong, S. H. Lee, and S.-J. Park, *Appl. Phys. Lett.*, **74**, 70 (1999).
4. J.-S. Jang, S.-J. Park, and T.-Y. Seong, *J. Vac. Sci. Technol. B*, **17**, 2667 (1999).
5. J. K. Kim, J. L. Lee, J. W. Lee, H. E. Shin, Y. J. Park, and T. I. Kim, *Appl. Phys. Lett.*, **73**, 2953 (1998).
6. J. K. Ho, C. S. Jong, C. C. Chiu, C. N. Huang, C. Y. Chen, and K. K. Shih, *Appl. Phys. Lett.*, **74**, 1275 (1999).
7. Y.-L. Li, E. F. Schubert, J. W. Graff, A. Osinsky, and W. F. Schaff, *Appl. Phys. Lett.*, **76**, 2728 (2000).
8. K. Kumakura, T. Makimoto, and N. Kobayashi, *Appl. Phys. Lett.*, **79**, 2588 (2001).
9. T. Gessmann, Y.-L. Li, E. L. Waldron, J. W. Graff, E. F. Schubert, and J. K. Sheu, *Appl. Phys. Lett.*, **80**, 986 (2002).
10. J.-S. Jang, S.-J. Sohn, D. Kim, and T.-Y. Seong, *Semicond. Sci. Technol.*, **21**, L37 (2006).
11. J.-S. Jang and T.-Y. Seong, *J. Appl. Phys.*, **101**, 013711 (2007).
12. J. Wu, *J. Appl. Phys.*, **106**, 011101 (2009).
13. E. F. Schubert, J. E. Cunningham, W. T. Tsang, and T. H. Chiu, *Appl. Phys. Lett.*, **49**, 292 (1986).
14. G. S. Marlow and M. B. Das, *Solid-State Electron.*, **25**, 91 (1982).
15. J.-S. Jang and T.-Y. Seong, *Appl. Phys. Lett.*, **91**, 092129 (2007).
16. J.-S. Jang and T.-Y. Seong, *Appl. Phys. Lett.*, **76**, 2743 (2000).
17. K. Kumakura, T. Makimoto, and N. Kobayahi, *Jpn. J. Appl. Phys., Part 1*, **42**, 2254 (2003).
18. F. R. de Boer, R. Boom, W. C. M. Mattens, A. R. Miedema, and A. K. Niessen, *Cohesion in Metals: Transition Metal Alloys*, North-Holland Physics, Amsterdam (1988).